

CHARMM-GUI PACE CG Builder for Solution, Micelle, and Bilayer Coarse-Grained Simulations

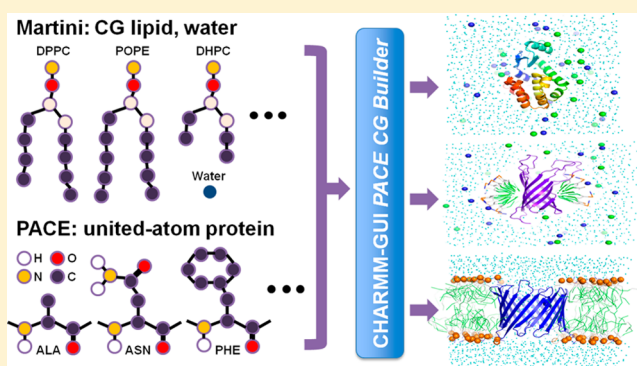
Yifei Qi,[†] Xi Cheng,[†] Wei Han,[‡] Sunhwan Jo,[†] Klaus Schulten,[‡] and Wonpil Im^{*,†}

[†]Department of Molecular Biosciences and Center for Bioinformatics, The University of Kansas, 2030 Becker Drive, Lawrence, Kansas 66047, United States

[‡]Beckman Institute and Center for Biophysics and Computational Biology, University of Illinois at Urbana–Champaign, Urbana, Illinois 61801, United States

S Supporting Information

ABSTRACT: Coarse-grained (CG) and multiscale simulations are widely used to study large biological systems. However, preparing the simulation system is time-consuming when the system has multiple components, because each component must be arranged carefully as in protein/micelle or protein/bilayer systems. We have developed CHARMM-GUI PACE CG Builder for building solution, micelle, and bilayer systems using the PACE force field, a united-atom (UA) model for proteins, and the Martini CG force field for water, ions, and lipids. The robustness of PACE CG Builder is validated by simulations of various systems in solution (α 3D, fibronectin, and lysozyme), micelles (Pf1, DAP12-NKG2C, OmpA, and DHPC-only micelle), and bilayers (GpA, OmpA, VDAC, MscL, OmpF, and lipid-only bilayers for six lipids). The micelle's radius of gyration, the bilayer thickness, and the per-lipid area in bilayers are comparable to the values from previous all-atom and CG simulations. Most tested proteins have root-mean squared deviations of less than 3 Å. We expect PACE CG Builder to be a useful tool for modeling/refining large, complex biological systems at the mixed UA/CG level.



INTRODUCTION

Molecular dynamics (MD) simulations are widely used to study biological systems that consist of protein, nucleic acids, lipids, and glycans. When the system size becomes intractable for all-atom simulation, coarse-grained (CG) and multiscale simulations are commonly used to average out some degrees of freedom in the system. Despite the paucity in molecular detail, CG simulations provide valuable information for understanding biological processes such as protein assembly,^{1–3} protein–protein interactions,^{4,5} protein folding,^{6,7} and membrane reactions.^{8–10} Moreover, incorporation of experimental data from methods such as FRET,¹¹ cryoEM,¹² and SAXS,¹³ greatly extends the capability of CG models to describe complex biological systems.

One popular CG force field (FF), known as Martini,¹⁴ maps on average four heavy atoms along with respective hydrogen atoms to one CG particle. The CG particles are classified into four main types—polar, nonpolar, apolar, and charged—and each main type is further classified based on its hydrogen-bonding capability or degree of polarity. The Martini FF was originally developed for lipids and later extended to include sugars¹⁵ and protein.¹⁶ However, the application of the Martini protein is limited to cases where details of conformational features are of little significance. Therefore, it is desirable to develop a hybrid model that accounts for proteins to a degree

of detail necessary for a CG description. One recent hybrid model of such kind is the PACE FF,^{17–19} which represents explicitly protein heavy atoms and polar hydrogen atoms (i.e., employs a united atom model). The PACE FF was parametrized in conjunction with Martini water and lipid, and it was shown to be able to fold small peptides and proteins and reproduce a variety of experimental observations.¹⁹

Although a combination of the Martini and PACE FFs holds great promise for simulations of proteins in heterogeneous environments, it is not trivial to construct heterogeneous systems for such simulations in a user-friendly manner. We note that there are scripts to generate Martini CG bilayers (<http://md.chem.rug.nl/cgmartini/index.php/tools2>) and PACE hybrid systems,¹⁹ but both scripts involve several programs. When a system has multiple components or involves a special arrangement (e.g., a micelle), using these scripts is challenging. While there are web-based user interfaces to build atomistic simulation systems,^{20–25} to the best of our knowledge, no such tool is available for the Martini/PACE hybrid model.

Here, we report the development of a web interface, CHARMM-GUI PACE CG Builder (<http://www.charmm-gui.org/input/cgbilayer> for bilayer builder), to simplify the building

Received: January 5, 2014

Published: March 4, 2014

of multiscale systems for PACE and Martini FF simulations in solution, micelle, and bilayer. We examined various simulation systems to demonstrate that PACE CG Builder is robust and that the software is well-suited for various types of simulations.

METHODS

Software Requirements. For lipid-only systems, NAMD 2.10 or a *nightly build version* is required to calculate the Martini Lennard-Jones switching energy correctly. For protein–lipid system, a modified version of NAMD is needed to deal with the nonbonded potentials designed for the PACE FF. This version of NAMD is available at the PACE CG Bilayer Builder front page (<http://www.charmm-gui.org/input/cgbilayer>).

PACE CG Builder. PACE CG Builder in CHARMM-GUI provides a separate submenu for *Solution Builder*, *Micelle Builder*, and *Bilayer Builder*. The overall processes of building solution, micelle, and bilayer CG simulation systems are identical to the corresponding all-atom builders (i.e., *Quick MD Simulator*,²¹ *Membrane Builder*,^{20,23} and *Micelle Builder*²⁵). Briefly, for PACE CG Bilayer Builder, a user can build a protein/bilayer complex or a bilayer-only system with single or multiple lipid types (see Figure 1 for the overall building process and Supporting Information Figures S1–3 for the screenshots of the web interface). Building and simulating the systems involve seven steps. In step 1, in the case of a protein/bilayer complex system, the protein structure can be read-in either from user input or the PDB²⁶/OPM database;²⁷ we note that the PDB structure from OPM is preoriented along the Z-axis, i.e., along the membrane normal, with the bilayer center at $Z = 0$. In step 2, the protein can be oriented if not aligned properly and pore water molecules can be added if necessary. In step 3, the system size is determined and the head groups of the lipids are packed using lipid-like pseudo atoms as described in detail in previous works^{20,23,25} (check *step3_packing.pdb* for lipid packing around a protein). The bilayer-only system building starts from step 3. In step 4, each component, such as water, ions, and lipids, is built separately. In step 5, all components previously built in step 4 are assembled, and the restraint and configuration files for NAMD are generated for

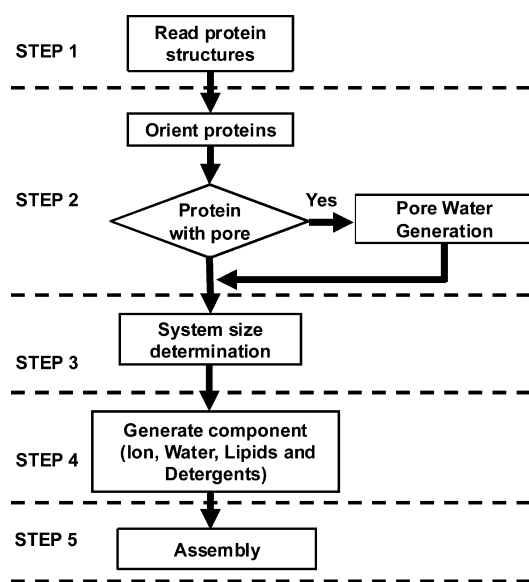


Figure 1. Procedure of system setup using PACE CG Micelle and Bilayer Builders.

Table 1. Lipid and Detergent Types Available in PACE CG Builder

name	full name	initial surface area (Å ²) ^a
DLPC	dilauroyl-phosphatidylcholine	57.2
DPPC	dipalmitoyl-phosphatidylcholine	63
DSPC	distearoyl-phosphatidylcholine	63
POPC	palmitoyl-oleoyl-phosphatidylcholine	68.3
DOPC	dioleoyl-phosphatidylcholine	67.4
DAPC	diarachidoyl-glycerophosphocholine	75
DLPE	dilauroyl-phosphatidylethanolamine	55
DPPE	dipalmitoyl-phosphatidylethanolamine	63
DSPE	distearoyl-phosphatidylethanolamine	63
POPE	palmitoyl-oleoyl-phosphatidylethanolamine	63
DOPE	dioleoyl-phosphatidylethanolamine	67.4
DHPC	diheptanoyl-phosphatidylcholine	50

^aThe initial surface area is used to estimate the number of lipids in bilayer and micelle system building. Data from ref 23.

equilibration (step 6) and production (step 7). Because the protein in the PACE FF has not been parametrized with phosphatidylglycerol (PG) and phosphatidylserine (PS) lipid types, only phosphatidylcholine (PC) and phosphatidylethanolamine (PE) lipid types are currently supported for protein/bilayer systems (see Table 1 for available PC and PE lipid types), and available ion types are limited to Na⁺ and Cl⁻.

For PACE CG Micelle Builder, all the building steps are similar to PACE CG Bilayer Builder except that detergents are used instead of lipids. Currently, only diheptanoyl-phosphatidylcholine (DHPC) is supported as a detergent. For PACE CG Solution Builder, the protein is solvated in step 2, and the periodic boundary condition is setup in step 3. NAMD inputs for equilibration (step 4) and production (step 5) are provided. The simulation protocol including the nonbonded interaction options is described below in detail.

The CHARMM²⁸ scripts for building the systems and the NAMD input files for equilibration and production are available to users. The CHARMM input files for simulations are not provided currently because the PACE FF uses 1–2 and 1–4 nonbonded interaction schemes at the same time, which is not implemented in CHARMM.

Test Systems. The PDB IDs of all the proteins used in this work are 2A3D (α 3D: a *de novo* designed single-chain three-helix bundle);²⁹ 2KBG (Fibronectin: the second Fibronectin type-III module of NCAM2); 2LZM (bacteriophage T4 lysozyme);³⁰ 2KSJ (Pf1 coat protein: the major coat protein of Pf1 bacteriophage);³¹ 2L35 (the DAP12-NKG2C transmembrane heterotrimer);³² 1G90 (OmpA: outer membrane protein A);³³ 1AFO (GpA: dimeric transmembrane domain of human glycoporphin A);³⁴ 2K4T (VDAC: the voltage-dependent anion channel);³⁵ 2OAR (MscL: mechanosensitive channel of large conductance);³⁶ and 2OMF (OmpF: outer membrane protein F). In DAP12-NKG2C, the aspartate residue (Asp16) in one of the DAP12 protomers, which faces out toward the bilayer hydrophobic core, was protonated, as in a previous study.³⁷ In GpA, only the transmembrane part was simulated with a sequence of Ace-ITLIIFGVMAGVIGTILLISYGI-NMe. The starting structures used in bilayer and micelle simulations were obtained from the OPM database.²⁷ All the systems were first neutralized with Na⁺ and Cl⁻ ions and buffered with 0.15 M NaCl solution. For solution and micelle systems, the system size was determined by extending 15 Å from each side of the

Table 2. Test Systems for the Solution, Micelle, and Bilayer Builders

builder	system	lipid number	system size (Å ³)	no. atoms
solution	α 3D	0	63 × 63 × 63	2565
solution	fibronectin	0	74 × 74 × 74	4100
solution	lysozyme	0	81 × 81 × 81	5626
micelle	DHPC	35	70 × 70 × 70	2789
micelle	Pfl + DHPC	75	83 × 83 × 83	5009
micelle	DAP12-NKG2C + DHPC	100	85 × 85 × 85	6029
micelle	OmpA + DHPC	80	87 × 87 × 87	6981
bilayer	DLPE	200	74 × 74 × 70	3290
bilayer	DLPC	200	75 × 75 × 70	3361
bilayer	DPPC	200	79 × 79 × 70	3647
bilayer	POPE	200	79 × 79 × 70	3896
bilayer	POPC	200	82 × 82 × 70	4027
bilayer	DOPC	200	82 × 82 × 70	4199
bilayer	GpA + POPC	160	74 × 74 × 83	4204
bilayer	OmpA + DOPE	200	87 × 87 × 93	7216
bilayer	VDAC + POPC	200	95 × 95 × 76	7614
bilayer	MscL + POPE	204	95 × 95 × 118	13222
bilayer	OmpF + POPC	226	112 × 112 × 88	16548

protein in the *X*, *Y*, and *Z* direction. In bilayer systems, the system size in the *XY* plane was determined to match the area of lipids and proteins, and a 15 Å water layer was added to each side of the bilayer.

Lipid Library. To sample the lipid structures effectively in the building process of a bilayer system, we used a lipid library that consists of 2000 configurations for each lipid type (Table 1), selected from a 100-ns simulation of a CG lipid bilayer. The bilayer system was simulated at 300 K with the presence of five molecules of each lipid type in each leaflet (one of the lipid layers). The frequency of saving the trajectory was 100 ps. After the principle geometric axis of each configuration was aligned to the *Z*-axis, the configurations with the first 2000 smallest radius of gyration on the *XY* plane were selected for the lipid library.

Simulation Protocol. For all micelle and bilayer systems, PACE CG Builder provides NAMD input files for the CHARMM-GUI standard six equilibration steps, during which the restraints on the lipid/detergent head groups and protein atoms are gradually reduced. As bilayers and micelles are modeled with MARTINI, calculation of nonbonded interactions for these systems follows a 1–2 rule, namely that nonbonded interactions are excluded if two interacting particles are separated at most by one bond. As for protein systems modeled with PACE, a 1–4 rule is applied to the calculation of nonbonded interactions. Thus, both rules are needed for systems with proteins in bilayers or micelles, which have been implemented in the modified NAMD as discussed above. For all systems, the electrostatic potential was evaluated by applying a shifting function between 0 and 12 Å. The dielectric constant was set to 15, the value used in PACE and MARTINI simulations. The nonbonded van der Waals interactions were calculated with a switching distance over 9–12 Å. The distance cutoff for searching for lists of interacting pairs was set to 14 Å. The time step was 20 fs for lipid-only systems³⁸ and 5 fs for protein-involved systems.¹⁹ All simulations here were performed in the NPT (constant number of particle, pressure, and temperature) ensemble. Temperature was controlled at 300 K with Langevin dynamics using a damping coefficient of 1 ps; pressure was controlled at 1.01325 bar with the Langevin piston Nose–Hoover method.^{39,40}

Trajectory Analysis. In lipid-only bilayer systems, the area per lipid was calculated by dividing the area in the *XY* plane by the number of lipids in one leaflet. The bilayer thickness was the distance between the average *Z* positions of the phosphate groups in each leaflet. The radius of gyration of micelle-containing systems was calculated with respect to phosphate atoms of detergent molecules. Root-mean squared deviation (RMSD) was calculated with respect to *C α* atoms in helices and β strands; in cases of membrane proteins, RMSD of their transmembrane part was evaluated. Trajectory analyses were performed using tools from CHARMM²⁸ and VMD.⁴¹

RESULTS AND DISCUSSION

In this section, we first validate that the Martini FF in the CHARMM format used in PACE CG Builder is accurate compared to the original FF in the Gromacs format. Then, the simulation results for 18 solution, micelle, and bilayer systems are presented and discussed in terms of RMSD, root-mean squared fluctuation (RMSF), radius of gyration, bilayer thickness, and per-lipid area.

Energy Comparison of Lipid-Only Bilayer Systems. As the Martini FF was originally developed in the framework of the simulation software package Gromacs,⁴² we converted the Martini FF to the CHARMM format to be used in the CHARMM-GUI framework. To validate the conversion, we compared the potential energies calculated using NAMD and Gromacs 4.5.5⁴² for one DHPC micelle and three lipid-only bilayer systems (Supporting Information Table S1). For these systems, the differences in bond, angle, van der Waals, and electrostatic energies from NAMD and Gromacs are very small, with a relative deviation of no more than 1.9×10^{-6} . The results demonstrate that the converted Martini FF is accurate enough to be used with NAMD to model systems with detergent/lipid as it is in Gromacs.

Simulation Examples of Solution, Micelle, and Bilayer Systems. To test PACE CG Builder and verify that the generated system and simulation files work properly, we performed 100-ns simulations of various solution, micelle, and bilayer systems with the number of atoms varying from \sim 2500 to \sim 16 500 (Table 2). For solution systems, the tested proteins are: α 3D (a small designed three-helix bundle protein),²⁹

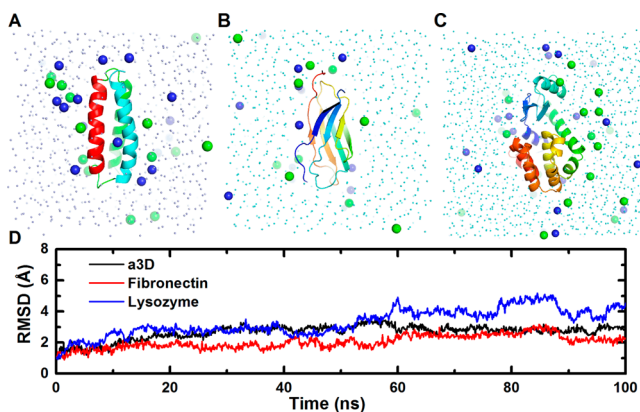


Figure 2. Solution systems of (A) α 3D, (B) fibronectin, (C) lysozyme, and (D) their RMSD time-series. Sodium and chloride ions are in blue and green spheres.

fibronectin (a protein with all- β structure), and lysozyme (a protein that is mostly helical).³⁰ The small RMSD ($< \sim 3$ Å) observed during the course of the 100-ns simulations indicates that the native structures of α 3D and fibronectin are well-maintained through the approach introduced in the current study (Figure 2). The lysozyme protein, however, is more flexible, reaching a RMSD of ~ 4 Å at the end of the 100-ns simulation. Visual inspection revealed that the conformational change corresponding to the maximal RMSD (~ 5 Å) involves the displacements of the helices from the amino- and carboxy-terminal domains (Supporting Information Figure S4). Such a change is consistent with the intrinsic hinge-bending motion of lysozyme in solution as seen in previous experiments.^{43,44}

To examine the capability of our approach for micelle systems, we tested four systems: a detergent-only system consisting of 65 DHPC; Pf1 (a coat protein from Pf1 bacteriophage);³¹ DAP12-NKG2C (the complex of the DAP12 signaling module and the natural killer cell-activating receptor NKG2C);³² OmpA (outer membrane protein A) (Figure 3).³³ The radius of gyration (R_g) of the head groups in the DHPC micelle is 21.0 ± 0.3 Å, in agreement with the result of a previous all-atom simulation (21.4 ± 0.2 Å).²⁵ In the protein systems, the R_g values did not fluctuate significantly, indicating overall stable protein/micelle complex structures. Pf1 and OmpA are very stable during the simulations, showing RMSD of less than 3 Å. To further evaluate if the simulations

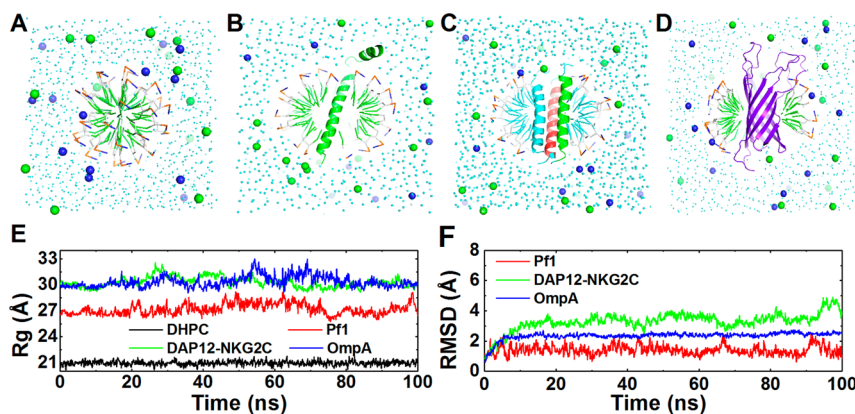


Figure 3. Micelle systems. (A) DHPC, (B) Pf1, (C) DAP12-NKG2C, (D) OmpA, (E) the time-series of radius of gyration of the detergent head groups, and (F) RMSD time-series of the proteins. Sodium and chloride ions are in blue and green spheres.

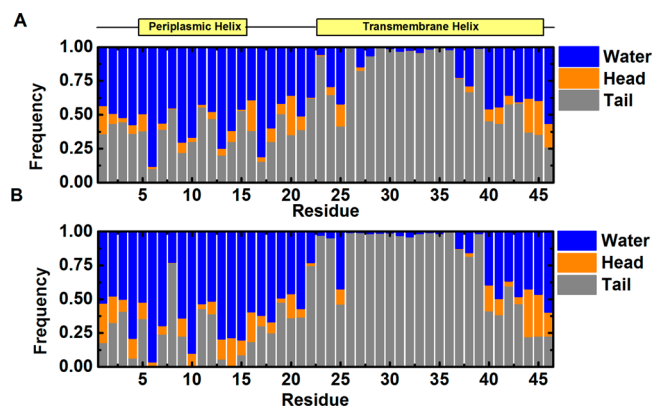


Figure 4. Contact frequency of residues in Pf1 to water, detergent head, and tail groups from (A) PACE CG and (B) all-atom simulations.²⁵ A contact is counted when the distance of a protein heavy atom to water/detergent is less than 5.5 Å.

reproduce properly the interactions between proteins and their heterogeneous environments, we calculated the contact frequency of each residue in Pf1 to water, detergent head, and tail groups (Figure 4). The transmembrane helix has higher frequency to interact with detergent tail groups than the periplasmic helix, in agreement with a previous all-atom simulation.²⁵ Compared to Pf1 and OmpA, DAP12-NKG2C shows larger fluctuations, with the largest RMSD approaching ~ 5 Å. Comparison of the final structure from the simulation to the initial structure reveals that the DAP12 dimer is distorted and rotated (Supporting Information Figure S5). Possible causes of such rearrangement are the polar residues (Asp16, Thr20, and Lys52) at the DAP12-NKG2C interface.³² In the NMR structure, Lys52 forms an electrostatic network with Asp16 and Thr20 from one DAP12 protomer. However, during the simulation, Asp16 and Thr20 from the other DAP12 protomer move inward and distort the helix, which was also observed in all-atom simulations (data not shown).³⁷

Finally, we extended our test to bilayer systems. We first tested six lipid-only bilayer systems, each consisting of 200 DLPC, DLPE, DPPC, POPC, POPE, and DOPC. The bilayer thickness and area per lipid of these systems did converge well (Table 3 and Supporting Information Figure S6). Moreover, the areas per lipid for all the systems are close to the results from previous CG simulations and experiments (Table 3). Five proteins, namely GpA, OmpA, VDAC, MscL, and OmpF, in

Table 3. Thickness and Area Per Lipid of Lipid-Only Bilayer Systems^a

lipid	thickness (Å)	area per lipid (Å ²)		
		current study	previous CG simulations ⁴⁶	experiment
DLPC	34.4 ± 0.3	60.1 ± 0.8	60	63 (303 K) ⁴⁷
DLPE	36.0 ± 0.3	55.3 ± 0.7	55	51 (308 K) ⁴⁸
DPPC	41.5 ± 0.4	60.2 ± 0.9	59	
POPC	42.6 ± 0.4	64.8 ± 0.9		64 (298 K) ⁴⁹
POPE	44.1 ± 0.4	61.2 ± 0.8	59	57 (303 K) ⁵⁰
DOPC	44.2 ± 0.4	68.0 ± 0.9	67	72 (303 K) ⁴⁸

^aThe current and previous CG simulations were all done at 300 K.

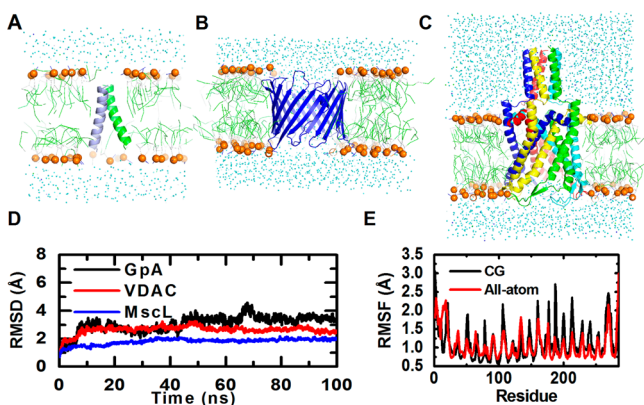


Figure 5. Bilayer systems. (A) GpA, (B) VDAC, (C) MscL, (D) their RMSD time-series, and (E) RMSF of VDAC from CG and a 65-ns all-atom simulation.⁵¹ Lipid phosphate atoms are in orange spheres. RMSF was calculated using the backbone non-hydrogen atoms.

different types of lipid bilayers were also tested. Except for GpA, the RMSDs of the proteins are smaller than 3 Å (Figure 5 and Supporting Information Figure S7). GpA has a slightly larger RMSD due to a 10° change in the crossing angle between the helices (Supporting Information Figure S8). In addition to protein stability, we also examined the dynamics of proteins in PACE CG simulations. Specifically, we analyzed the RMSF of VDAC for which the same analysis of all-atom simulations is available. As shown in Figure 5E, the RMSFs arising from the PACE CG and all-atom simulations are very similar, particularly for the regions where secondary structures are formed. Interestingly, the loop regions exhibit larger RMSF values for the CG simulation, suggesting that more conformational variations in these regions are sampled. As the PACE FF often leads to simulations with dynamics faster than those using all-atom FF by about 1 order of magnitude,¹⁹ our current 100-ns simulation may allow us to observe the dynamics that actually requires microsecond-long simulations in the all-atom case.

Table 4. Speed Comparison of PACE CG and All-Atom Simulation^a

system	PACE CG			All-atom			speed up
	box size (Å ³)	atom number	speed (ns/day)	box size (Å ³)	atom number	speed (ns/day)	
α3d	63 × 63 × 63	2565	40.0	63 × 63 × 63	24702	1.4	28
Pfl	83 × 83 × 83	5009	26.3	83 × 83 × 83	53753	0.7	37
VDAC	95 × 95 × 76	7614	17.2	95 × 95 × 76	65033	0.6	28

^aThe all-atom systems were built to match the box size of the CG systems with the same number of lipids or detergents. Simulations were performed on a 2.83 GHz Intel Xeon CPU using four cores.

CONCLUSION

In this study, we developed and tested the CHARMM-GUI PACE CG Builder, a web-based user interface for building solution, micelle, and bilayer PACE CG simulation systems. A total of 18 different systems were investigated in regard to structural stability during their simulations. Most proteins have RMSD values of less than 3 Å, and the radius of gyration, the bilayer thickness, and the area per lipid are similar to those from previous simulations. With the Martini CG FF, the number of atoms in a simulation system can be reduced by a factor of 10. Considering that a time step of 5 fs is used in the PACE/Martini hybrid simulation, about 30-times increase in simulation performance can be achieved compared to all-atom simulations using a 2-fs time step (Table 4). Finally, the PACE FF provides more details for the protein than the Martini protein model, which is a superior feature in applications such as structural refinement.⁴⁵ We expect PACE CG Builder to be a useful tool for studying solution, micelle, and bilayer systems at the united-atom and CG level.

ASSOCIATED CONTENT

Supporting Information

Screenshots of the PACE CG builder web interface (Figures S1–3). Comparison of the last snapshot from MD to the crystal structure of lysozyme (Figure S4). Comparison of the last snapshot from MD to the NMR structure of DAP12-NKG2C (Figure S5). Thickness and area per lipid of bilayer systems (Figure S6). Structure and RMSD time-series of OmpA and OmpF in bilayer (Figure S7). The conformation of GpA during simulation (Figure S8). Validation of the converted MARTINI force field (Table S1). This material is available free of charge via the Internet at <http://pubs.acs.org>.

AUTHOR INFORMATION

Corresponding Author

*Phone: (785) 864-1993. Fax: (785) 864-5558. E-mail: wonpil@ku.edu.

Notes

The authors declare no competing financial interest.

ACKNOWLEDGMENTS

This work was supported in part by NSF ABI-1145987, NIH U54GM087519, and XSEDE TG-MCB070009 (to WI).

REFERENCES

- Arhipov, A.; Freddolino, P. L.; Schulten, K. Stability and Dynamics of Virus Capsids Described by Coarse-Grained Modeling. *Structure* **2006**, *14*, 1767–1777.
- Nguyen, H. D.; Reddy, V. S.; Brooks, C. L., 3rd Invariant Polymorphism in Virus Capsid Assembly. *J. Am. Chem. Soc.* **2009**, *131*, 2606–2614.

- (3) Ayton, G. S.; Voth, G. A. Multiscale Computer Simulation of the Immature HIV-1 Virion. *Biophys. J.* **2010**, *99*, 2757–2765.
- (4) Hall, B. A.; Armitage, J. P.; Sansom, M. S. Mechanism of Bacterial Signal Transduction Revealed by Molecular Dynamics of Tsr Dimers and Trimers of Dimers in Lipid Vesicles. *PLoS Comput. Biol.* **2012**, *8*, e1002685.
- (5) Janosi, L.; Li, Z.; Hancock, J. F.; Gorfe, A. A. Organization, Dynamics, and Segregation of Ras Nanoclusters in Membrane Domains. *Proc. Natl. Acad. Sci. USA* **2012**, *109*, 8097–8102.
- (6) Qi, Y.; Huang, Y.; Liang, H.; Liu, Z.; Lai, L. Folding Simulations of a De Novo Designed Protein with a Betaalphabet Fold. *Biophys. J.* **2010**, *98*, 321–329.
- (7) Zhang, Z.; Chan, H. S. Competition between Native Topology and Nonnative Interactions in Simple and Complex Folding Kinetics of Natural and Designed Proteins. *Proc. Natl. Acad. Sci. USA* **2010**, *107*, 2920–2925.
- (8) Marrink, S. J.; de Vries, A. H.; Tieleman, D. P. Lipids on the Move: Simulations of Membrane Pores, Domains, Stalks and Curves. *Biochim. Biophys. Acta* **2009**, *1788*, 149–168.
- (9) Wu, Z.; Cui, Q.; Yethiraj, A. Why Do Arginine and Lysine Organize Lipids Differently? Insights from Coarse-Grained and Atomistic Simulations. *J. Phys. Chem. B* **2013**, *117*, 12145–12156.
- (10) Yoo, J.; Jackson, M. B.; Cui, Q. A Comparison of Coarse-Grained and Continuum Models for Membrane Bending in Lipid Bilayer Fusion Pores. *Biophys. J.* **2013**, *104*, 841–852.
- (11) Marius, P.; Leung, Y. M.; Piggot, T. J.; Khalid, S.; Williamson, P. T. Probing the Oligomeric State and Interaction Surfaces of Fukutin-I in Dilauroylphosphatidylcholine Bilayers. *Eur. Biophys. J.* **2012**, *41*, 199–207.
- (12) Grubisic, I.; Shokhiev, M. N.; Orzechowski, M.; Miyashita, O.; Tama, F. Biased Coarse-Grained Molecular Dynamics Simulation Approach for Flexible Fitting of X-Ray Structure into Cryo Electron Microscopy Maps. *J. Struct. Biol.* **2010**, *169*, 95–105.
- (13) Yang, S.; Blachowicz, L.; Makowski, L.; Roux, B. Multidomain Assembled States of Hck Tyrosine Kinase in Solution. *Proc. Natl. Acad. Sci. USA* **2010**, *107*, 15757–15762.
- (14) Marrink, S. J.; Risselada, H. J.; Yefimov, S.; Tieleman, D. P.; de Vries, A. H. The Martini Force Field: Coarse Grained Model for Biomolecular Simulations. *J. Phys. Chem. B* **2007**, *111*, 7812–7824.
- (15) López, C. A.; Rzeplia, A. J.; de Vries, A. H.; Dijkhuizen, L.; Hünenberger, P. H.; Marrink, S. J. Martini Coarse-Grained Force Field: Extension to Carbohydrates. *J. Chem. Theory Comput.* **2009**, *5*, 3195–3210.
- (16) Monticelli, L.; Kandasamy, S. K.; Periole, X.; Larson, R. G.; Tieleman, D. P.; Marrink, S. J. The Martini Coarse-Grained Force Field: Extension to Proteins. *J. Chem. Theory Comput.* **2008**, *4*, 819–834.
- (17) Han, W.; Wan, C.-K.; Jiang, F.; Wu, Y.-D. Pace Force Field for Protein Simulations. 1. Full Parameterization of Version 1 and Verification. *J. Chem. Theory Comput.* **2010**, *6*, 3373–3389.
- (18) Han, W.; Wan, C.-K.; Wu, Y.-D. Pace Force Field for Protein Simulations. 2. Folding Simulations of Peptides. *J. Chem. Theory Comput.* **2010**, *6*, 3390–3402.
- (19) Han, W.; Schulten, K. Further Optimization of a Hybrid United-Atom and Coarse-Grained Force Field for Folding Simulations: Improved Backbone Hydration and Interactions between Charged Side Chains. *J. Chem. Theory Comput.* **2012**, *8*, 4413–4424.
- (20) Jo, S.; Kim, T.; Im, W. Automated Builder and Database of Protein/Membrane Complexes for Molecular Dynamics Simulations. *PLoS One* **2007**, *2*, e880.
- (21) Jo, S.; Kim, T.; Iyer, V. G.; Im, W. Charmm-Gui: A Web-Based Graphical User Interface for Charmm. *J. Comput. Chem.* **2008**, *29*, 1859–1865.
- (22) Miller, B. T.; Singh, R. P.; Klauda, J. B.; Hodoscek, M.; Brooks, B. R.; Woodcock, H. L., 3rd. Charmm: A New, Flexible Web Portal for Charmm. *J. Chem. Inf. Model* **2008**, *48*, 1920–1929.
- (23) Jo, S.; Lim, J. B.; Klauda, J. B.; Im, W. Charmm-Gui Membrane Builder for Mixed Bilayers and Its Application to Yeast Membranes. *Biophys. J.* **2009**, *97*, 50–58.
- (24) van Dijk, M.; Wassenaar, T. A.; Bonvin, A. M. J. J. A Flexible, Grid-Enabled Web Portal for Gromacs Molecular Dynamics Simulations. *J. Chem. Theory Comput.* **2012**, *8*, 3463–3472.
- (25) Cheng, X.; Jo, S.; Lee, H. S.; Klauda, J. B.; Im, W. Charmm-Gui Micelle Builder for Pure/Mixed Micelle and Protein/Micelle Complex Systems. *J. Chem. Inf. Model* **2013**, *53*, 2171–2180.
- (26) Bernstein, F. C.; Koetzle, T. F.; Williams, G. J.; Meyer, E. F., Jr.; Brice, M. D.; Rodgers, J. R.; Kennard, O.; Shimanouchi, T.; Tasumi, M. The Protein Data Bank. A Computer-Based Archival File for Macromolecular Structures. *Eur. J. Biochem.* **1977**, *80*, 319–324.
- (27) Lomize, M. A.; Lomize, A. L.; Pogozheva, I. D.; Mosberg, H. I. Opm: Orientations of Proteins in Membranes Database. *Bioinformatics* **2006**, *22*, 623–625.
- (28) Brooks, B. R.; Brooks, C. L., 3rd; Mackerell, A. D., Jr.; Nilsson, L.; Petrella, R. J.; Roux, B.; Won, Y.; Archontis, G.; Bartels, C.; Boresch, S.; Caffisch, A.; Caves, L.; Cui, Q.; Dinner, A. R.; Feig, M.; Fischer, S.; Gao, J.; Hodoscek, M.; Im, W.; Kuczera, K.; Lazaridis, T.; Ma, J.; Ovchinnikov, V.; Paci, E.; Pastor, R. W.; Post, C. B.; Pu, J. Z.; Schaefer, M.; Tidor, B.; Venable, R. M.; Woodcock, H. L.; Wu, X.; Yang, W.; York, D. M.; Karplus, M. Charmm: The Biomolecular Simulation Program. *J. Comput. Chem.* **2009**, *30*, 1545–1614.
- (29) Walsh, S. T.; Cheng, H.; Bryson, J. W.; Roder, H.; DeGrado, W. F. Solution Structure and Dynamics of a De Novo Designed Three-Helix Bundle Protein. *Proc. Natl. Acad. Sci. USA* **1999**, *96*, 5486–5491.
- (30) Weaver, L. H.; Matthews, B. W. Structure of Bacteriophage T4 Lysozyme Refined at 1.7 Å Resolution. *J. Mol. Biol.* **1987**, *193*, 189–199.
- (31) Park, S. H.; Marassi, F. M.; Black, D.; Opella, S. J. Structure and Dynamics of the Membrane-Bound Form of Pfl Coat Protein: Implications of Structural Rearrangement for Virus Assembly. *Biophys. J.* **2010**, *99*, 1465–1474.
- (32) Call, M. E.; Wucherpfennig, K. W.; Chou, J. J. The Structural Basis for Intramembrane Assembly of an Activating Immunoreceptor Complex. *Nat. Immunol.* **2010**, *11*, 1023–1029.
- (33) Arora, A.; Abildgaard, F.; Bushweller, J. H.; Tamm, L. K. Structure of Outer Membrane Protein a Transmembrane Domain by Nmr Spectroscopy. *Nat. Struct. Biol.* **2001**, *8*, 334–338.
- (34) MacKenzie, K. R.; Prestegard, J. H.; Engelman, D. M. A Transmembrane Helix Dimer: Structure and Implications. *Science* **1997**, *276*, 131–133.
- (35) Hiller, S.; Garces, R. G.; Malia, T. J.; Orekhov, V. Y.; Colombini, M.; Wagner, G. Solution Structure of the Integral Human Membrane Protein Vdac-1 in Detergent Micelles. *Science* **2008**, *321*, 1206–1210.
- (36) Steinbacher, S.; Bass, R.; Strop, P.; Rees, D. C. Structures of the Prokaryotic Mechanosensitive Channels Mscl and Mscl. *Curr. Top. Membr.* **2007**, *58*, 1–24.
- (37) Cheng, X.; Im, W. Nmr Observable-Based Structure Refinement of Dap12-Nkg2c Activating Immunoreceptor Complex in Explicit Membranes. *Biophys. J.* **2012**, *102*, L27–29.
- (38) de Jong, D. H.; Singh, G.; Bennett, W. F. D.; Arnarez, C.; Wassenaar, T. A.; Schafer, L. V.; Periole, X.; Tieleman, D. P.; Marrink, S. J. Improved Parameters for the Martini Coarse-Grained Protein Force Field. *J. Chem. Theory Comput.* **2013**, *9*, 687–697.
- (39) Martyna, G. J.; Tobias, D. J.; Klein, M. L. Constant-Pressure Molecular-Dynamics Algorithms. *J. Chem. Phys.* **1994**, *101*, 4177–4189.
- (40) Feller, S. E.; Zhang, Y. H.; Pastor, R. W.; Brooks, B. R. Constant-Pressure Molecular-Dynamics Simulation - the Langevin Piston Method. *J. Chem. Phys.* **1995**, *103*, 4613–4621.
- (41) Humphrey, W.; Dalke, A.; Schulten, K. Vmd: Visual Molecular Dynamics. *J. Mol. Graph.* **1996**, *14*, 33–38.
- (42) Pronk, S.; Pall, S.; Schulz, R.; Larsson, P.; Bjelkmar, P.; Apostolov, R.; Shirts, M. R.; Smith, J. C.; Kasson, P. M.; van der Spoel, D.; Hess, B.; Lindahl, E. Gromacs 4.5: A High-Throughput and Highly Parallel Open Source Molecular Simulation Toolkit. *Bioinformatics* **2013**, *29*, 845–854.
- (43) Faber, H. R.; Matthews, B. W. A Mutant T4 Lysozyme Displays Five Different Crystal Conformations. *Nature* **1990**, *348*, 263–266.

- (44) McHaourab, H. S.; Oh, K. J.; Fang, C. J.; Hubbell, W. L. Conformation of T4 Lysozyme in Solution. Hinge-Bending Motion and the Substrate-Induced Conformational Transition Studied by Site-Directed Spin Labeling. *Biochemistry* **1997**, *36*, 307–316.
- (45) Trabuco, L. G.; Villa, E.; Mitra, K.; Frank, J.; Schulten, K. Flexible Fitting of Atomic Structures into Electron Microscopy Maps Using Molecular Dynamics. *Structure* **2008**, *16*, 673–683.
- (46) Marrink, S. J.; de Vries, A. H.; Mark, A. E. Coarse Grained Model for Semiquantitative Lipid Simulations. *J. Phys. Chem. B* **2004**, *108*, 750–760.
- (47) Petrache, H. I.; Dodd, S. W.; Brown, M. F. Area Per Lipid and Acyl Length Distributions in Fluid Phosphatidylcholines Determined by $(2)H$ Nmr Spectroscopy. *Biophys. J.* **2000**, *79*, 3172–3192.
- (48) Nagle, J. F.; Tristram-Nagle, S. Structure of Lipid Bilayers. *Biochim. Biophys. Acta* **2000**, *1469*, 159–195.
- (49) Konig, B.; Dietrich, U.; Klose, G. Hydration and Structural Properties of Mixed Lipid/Surfactant Model Membranes. *Langmuir* **1997**, *13*, 525–532.
- (50) Rand, R. P.; Parsegian, V. A. Hydration Forces between Phospholipid-Bilayers. *Biochim. Biophys. Acta* **1989**, *988*, 351–376.
- (51) Rui, H.; Lee, K. I.; Pastor, R. W.; Im, W. Molecular Dynamics Studies of Ion Permeation in Vdac. *Biophys. J.* **2011**, *100*, 602–610.